Observation of Surface States with Algebraic Localization

G. Corrielli,[1,2] G. Della Valle,[1,2] A. Crespi,[2,1] R. Osellame,[2,1] and S. Longhi[1,2,*]

[1]*Dipartimento di Fisica-Politecnico di Milano, Piazza Leonardo da Vinci 32, 20133 Milan, Italy*

[2]*Istituto di Fotonica e Nanotecnologie-Consiglio Nazionale delle Ricerche, Piazza Leonardo da Vinci 32, 20133 Milan, Italy*

(Received 4 June 2013; published 26 November 2013)

We introduce and experimentally demonstrate a class of surface bound states with algebraic decay in a one-dimensional tight-binding lattice. Such states have an energy embedded in the spectrum of scattered states and are structurally stable against perturbations of lattice parameters. Experimental demonstration of surface states with algebraic localization is presented in an array of evanescently coupled optical waveguides with tailored coupling rates.

DOI: 10.1103/PhysRevLett.111.220403 PACS numbers: 03.65.Nk, 03.65.Ge, 42.82.Et, 73.20.At

Surface waves localized at an interface between two different media play an important role in different areas of physics [1]. A widespread belief is that surface waves are exponentially localized waves. Indeed, exponential localization is ubiquitous for evanescent waves. Exponential localization is found for electrons at the surface of a periodic crystal, the so-called Tamm [2] and Shockley [3] surface states with energy in a gap, in disordered lattices, as a result of Anderson localization [4], or at a metal-dielectric interface in the form of plasmonic waves. However, quantum mechanics does not exclude the existence of localized states with a *lower* than exponential localization. Subexponential localization, including a power-law decay of the wave function, can arise, for example, in lattice models with special kinds of disorder [5,6]. Surface states with algebraic localization were predicted 20 years ago in certain special potentials for the Schrödinger equation on a semi-infinite line [7]. Such surface states have an energy embedded in the continuous spectrum of scattered states; i.e., they belong to the class of bound states in the continuum (BIC) originally discovered by von Neumann and Wigner in a seminal paper [8] and found in a wide range of quantum and classical systems, including atomic and molecular systems [9–11], semiconductor and mesoscopic structures [12–17], graphene [18], quantum Hall insulators [19], Hubbard models [20,21], and optical structures [22–26]. Experimental demonstrations of BIC states, either in the bulk [25] or at the surface [26], have been recently reported in simple optical lattice systems exploiting destructive Fano interference. Such BIC states are compact; i.e., they confine all the energy in few sites with no penetration into the lattice continuum and are thus not suited to observe subexponential localization. Recently, surface states with subexponential localization have been theoretically introduced by Molina and coworkers in a special tight-binding lattice model [27]. Such states are BIC modes which, as opposed to those earlier studied in Refs. [22,25,26], are not compact and penetrate in the lattice with a subexponential (but higher than algebraic) localization. However, like in [7] a specially tailored local potential is required, which is of difficult experimental implementation. The observation of surface states with subexponential localization remains to date elusive.

In this Letter we introduce and experimentally demonstrate surface states with power-law decay in a semi-infinite tight-binding lattice model, which do not require any local potential. Algebraic localization exploits the existence of a BIC mode, and it is not related to a special kind of disorder in the lattice [5,6]. Our scheme is experimentally demonstrated in an array of coupled optical waveguides with tailored hopping rates, manufactured by femtosecond laser writing in fused silica. Algebraic localization of the surface state is proven by spectral reconstruction of the BIC eigenmode from beam propagation measurements.

We consider a semi-infinite tight-binding lattice with inhomogeneous hopping rates κ_n and site energies ϵ_n ($n = 1, 2, 3, \ldots$) described by the tight-binding Hamiltonian

$$\hat{H} = -\sum_{n=1}^{\infty} \{\kappa_n |n\rangle\langle n+1| + \kappa_{n-1} |n\rangle\langle n-1|\} + \sum_{n=1}^{\infty} \epsilon_n |n\rangle\langle n|, \quad (1)$$

where $\kappa_n > 0$ is the hopping rate between sites $|n\rangle$ and $|n+1\rangle$, and $\kappa_0 = 0$. We assume that, far from $n = 1$, the lattice is homogeneous, i.e., $\epsilon_n \to 0$ and $\kappa_n \to \kappa$ as $n \to \infty$. The energy spectrum of $\hat{H}$ is obtained from the following eigenvalue equation for the occupation amplitudes $\bar{c}_n$ of various lattice sites,

$$E\bar{c}_n = -\kappa_n \bar{c}_{n+1} - \kappa_{n-1}\bar{c}_{n-1} + \epsilon_n \bar{c}_n, \quad (2)$$

where $n = 1, 2, 3, \ldots$. The linear spectrum of scattered states, i.e., the continuous spectrum of $\hat{H}$, is provided by the tight-binding lattice band $-2\kappa < E < 2\kappa$. Bound states can arise owing to the inhomogeneity of the hopping rates κ_n and/or of the local potential ϵ_n. A method to create a single BIC surface state in a lattice with $\kappa_n = \kappa$ and with

a specially tailored local potential ϵ_n was proposed in Ref. [27]. Here we suggest a different and experimentally more accessible method to synthesize a discrete lattice that sustains an arbitrary number $M \geq 1$ of surface BIC with algebraic localization that does not require any local potential, i.e., $\epsilon_n = 0$. Our idea is to introduce a modulation of the hopping rates κ_n between adjacent sites, which can be simply realized in a semi-infinite tight-binding lattice with inhomogeneous spacing of adjacent lattice sites. Some general properties of the Hamiltonian $\hat{H}$ in the $\epsilon_n = 0$ case and for inhomogeneous hopping rates are discussed in the Supplemental Material [28]. To realize a BIC state with algebraic localization, let us modulate the lattice hopping rates κ_n as follows,

$$\kappa_n = \begin{cases} \kappa & n \neq lN \\ \left(\frac{l+1}{l}\right)^{\beta} \kappa & n = lN (l = 1, 2, 3, \ldots) \end{cases}, \tag{3}$$

where $N = M + 1$ and β is an arbitrary real number that defines the power-law decay exponent ($\beta > 1/2$ for normalizable states). Indeed, it can be readily shown that Eqs. (2) admit the following M surface states,

$$\bar{c}_n^{(\sigma)} = A_n \sin(n q_\sigma), \tag{4}$$

with energies $E_\sigma = -2\kappa \cos q_\sigma$ buried in the band of scattered states. In the previous equation, $\sigma = 1, 2, \ldots, M$, $q_\sigma = \pi\sigma/N$, $A_n = \mathcal{N} l^{-\beta}$ for $(l-1)N < n \leq lN$ ($l = 1, 2, 3, \ldots$), and $\mathcal{N}$ is a normalization constant. As an example, in Fig. 1(a) we show the very simple discrete lattice that sustains one surface BIC with the algebraic decay law $\bar{c}_n \sim 2/(n+1)$, i.e., corresponding to $N = 2$ and $\beta = 1$, with energy $E = 0$ at the center of the tight-binding lattice band. The distribution of the surface BIC is depicted in Fig. 1(b). In addition to surface BIC, the lattices defined by the sequence (3) sustain additional surface states in the gap, i.e., bound states outside the continuum (BOC). As an example, in Fig. 1(c) we show the numerically computed energy spectrum of Eq. (2) in a lattice comprising $N_s = 501$ sites for $N = 2$ and $\beta = 1$, i.e., for the lattice shown in Fig. 1(a). The degree of localization of the eigenstate $\bar{c}_n(E)$ with energy E is measured by the participation ratio $R(E)$, given by $R(E) = (\sum_n |\bar{c}_n|^2)^2/(\sum_n |\bar{c}_n|^4)$ [27]. For localized modes, $R \sim 1$ while for extended states $R \sim N_s$. The distribution of $R(E)$ for the $N_s = 501$ eigenmodes of the lattice of Fig. 1(a) is shown in Fig. 1(d). The figure clearly shows the existence of one BIC surface state at $E = 0$, together with a number of BOC surface states (26 for the truncated lattice with $N_s = 501$ sites) with exponential decay tails and with energies outside the lattice band. The two outer BOC states have an energy $E \sim \pm E_0 \simeq \pm 2.56\kappa$, whereas the energies of the other BOC modes condensate toward the band gap edges $E = \pm 2\kappa$. The surface BIC turns out to be structurally robust against perturbations of lattice parameters, as discussed in Ref. [28].

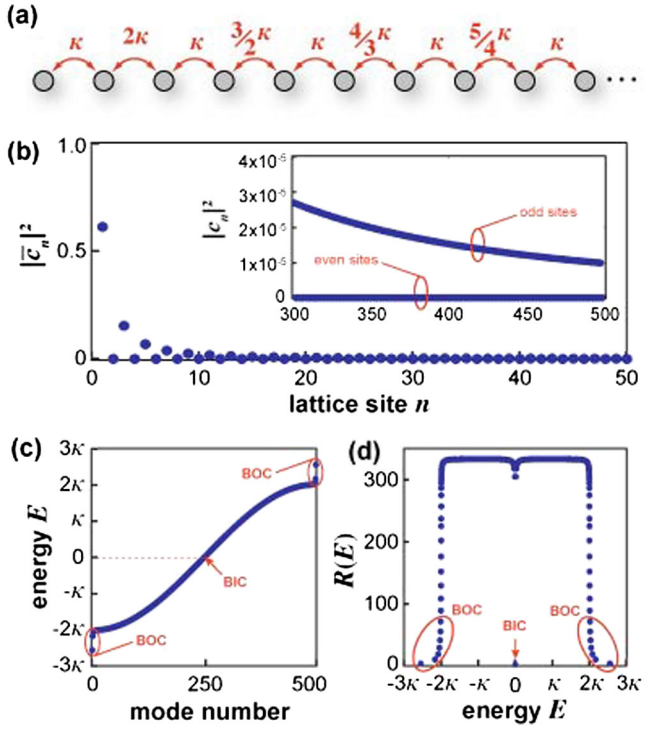

FIG. 1 (color online). (a) Schematic of a semi-infinite lattice with tailored hopping rates that sustains $M = 1$ BIC surface state with algebraic decay ($\beta = 1$). (b) Behavior of $|\bar{c}_n|^2$ for the BIC state. (c) Numerically computed energy spectrum of the lattice comprising $N_s = 501$ sites, and (d) corresponding behavior of the participation ratio $R(E)$ of the eigenmodes. The BIC state has an energy $E = 0$. BOC modes are located close to the band gap edges $\pm 2\kappa$. The outer BOC modes have an energy $E = \pm E_0 \simeq \pm 2.557\kappa$.

To experimentally demonstrate surface BIC modes, we implemented the semi-infinite lattice of Fig. 1(a) in an array of 40 evanescently coupled optical waveguides manufactured by femtosecond laser waveguide writing on a fused silica substrate (see, for instance, [29,30]). The second harmonic of a Yb-based femtosecond laser (FemtoREGEN, HighQLaser GmbH), delivering 400 fs pulses, is used for the writing process. An optimal processing window was found at 20 kHz repetition rate, 300 nJ pulse energy, and 10 mm/s translation speed. The laser beam is focused at 170 μm below the glass surface by a 0.45 NA, 20 × objective. The spacing d_n between waveguide $|n\rangle$ and $|n+1\rangle$ is engineered in order to implement the desired coupling coefficients, namely $\kappa_n/\kappa = 1, 2, 1, 3/2, 1, 4/3, 1, 5/4, \ldots$. For our waveguide writing parameters, the coupling constant κ_n turns out to be well fitted by the exponential curve $\kappa_n = \kappa \exp[-\gamma(d_n - a)]$, where $\kappa = 1.27$ cm^{-1} is the coupling constant for a waveguide spacing $a = 15$ μm and $\gamma = 0.20$ μm^{-1}. The values of κ_n of the lattice of Fig. 1(a) are obtained with spacings in the range $d_n = 11.5$–15 μm. The array was probed at $\lambda = 633$ nm from light emitted by a He-Ne laser. Note that in our optical setting the spatial light propagation

along the axial distance z of the array reproduces the temporal evolution of the occupation amplitudes $c_n(t)$ in the lattice model described by the Hamiltonian (1), with $t = z$. To prove the existence of the surface BIC mode with algebraic localization, we measured the propagation of a light beam in the arrayed structure under suitable excitation at the input plane and used a spectral method to reconstruct the eigenenergy and profile of the BIC mode [31]. The method basically requires us to measure the correlation function $C(t)$ of the evolving optical wave packet $|\psi(n,t)\rangle = \sum_n c_n(t)|n\rangle$, i.e., $C(t) = \langle\psi(0)|\psi(t)\rangle$, and the evolution of $c_n(t)$ in the various lattice sites. Fourier analysis of the correlation function enables us to localize the position of the discrete eigenvalues as resonance peaks, whereas a Fourier analysis of $|\psi(n,t)\rangle$ generates the eigenfunction profiles [31]. Technical details of the spectral method are given in Ref. [28]. To correctly reconstruct the eigenvector corresponding to the BIC state of the Hamiltonian (1), two conditions should be met: (1) the initial wave packet should have a non-negligible overlap with the BIC mode and (2) the wave packet evolution should be monitored for a time T much longer than $\sim 1/\kappa$. The latter condition arises because the BIC state is embedded into the spectrum of scattered states, whose contribution into the reconstructed state should be avoided. Once the two conditions (1) and (2) are met, the energy position $E = E_1$ of the BIC state is found as a resonance peak of the Fourier transform $\hat{C}(E)$ of $C(t)$, i.e.,

$$\hat{C}(E) = \int_{-\infty}^{\infty} dt g(t)\langle\psi(0)|\psi(t)\rangle \exp(iEt), \tag{5}$$

whereas the corresponding eigenvector, apart from a normalization factor, is reconstructed via the relation

$$\bar{c}_n(E_1) \simeq \int_{-\infty}^{\infty} dt g(t) c_n(t) \exp(iE_1 t). \tag{6}$$

In Eqs. (5) and (6), $g(t)$ is a window function of length $\sim T$, which can be chosen to be a Gaussian or a square-wave function [28,31]. Its Fourier transform is the spectral filtering function, whose spectral width $\sim 1/T$ sets the minimum separation in energy levels that can be resolved [31]. In our experiment, to meet the above-mentioned conditions we propagated light along the array for a distance of 9 cm, corresponding to a time $T \simeq 11.4/\kappa$, and excited the system at the left boundary waveguide $n = 1$ [see red arrow in Fig. 2(a)], corresponding to the initial wave packet $|\psi(n,0)\rangle = |1\rangle$. For such an initial condition, the various lattice eigenmodes are excited with a weight $A(E)$ which is depicted in Fig. 2(b). The figure clearly shows that the BIC state with energy $E = 0$ is the most excited eigenstate, and the condition (1) above is met. Moreover, the propagated time $T \simeq 11.4/\kappa$ is long enough to provide a satisfactory resolution of the BIC eigenvalue and a negligible contribution of the scattered states in the reconstruction of the BIC mode profile [28], according to the condition (2). As discussed in Ref. [28], for the lattice Hamiltonian (1) with $\epsilon_n = 0$ and for the chosen initial condition, $c_n(t)$ turns out to be either real-valued or purely imaginary-valued. Such a property greatly simplifies the experiment because a measurement of the light intensity distributions $|c_n(t)|^2$ is sufficient to retrieve the behavior of $c_n(t)$, and hence the computation of the correlation function and reconstruction of the eigenvector according to Eqs. (5) and (6). In our experiment, the evolution of $|c_n(t)|^2$ was measured by top-view imaging of the fluorescence signal emitted by the waveguides where red light is propagating [30,32,33]; further details are given in Ref. [28]. In Fig. 2(c) we show the measured map of light intensity evolution along the 9-cm-long waveguide array. For comparison, the corresponding theoretical map is also shown in Fig. 2(d). Note the good agreement between the two maps. From the measured intensity map, we extracted the evolution of $c_n(t)$ in the various guides [28] and computed the spectrum of the correlation function using a Gaussian filter $g(t) = g_G(t) = (1/T)\exp[-(t - T/2)^2/w^2]$, truncated at $t < 0$ and $t > T$, with $w = 2T/5$. As compared to

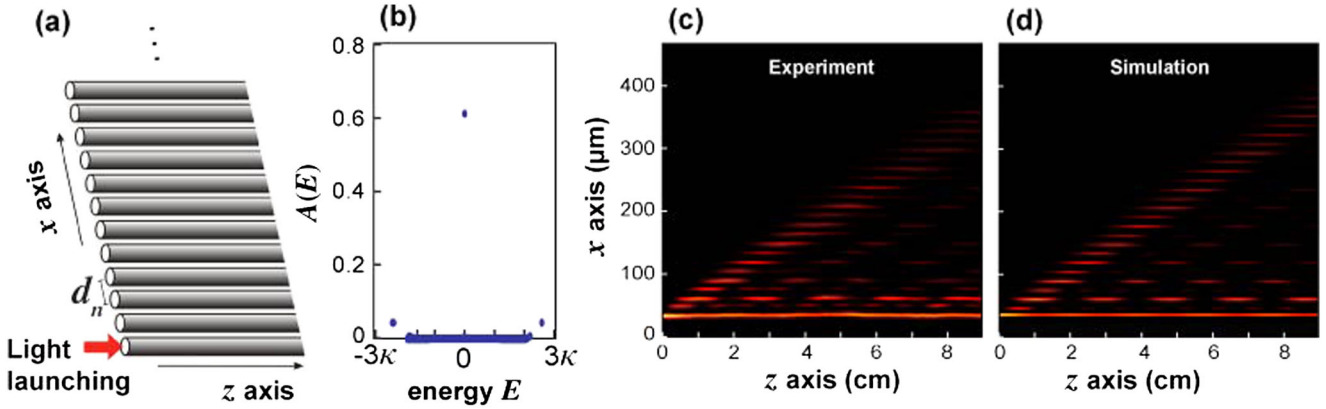

FIG. 2 (color online). (a) Schematic of the waveguide lattice; the red arrow indicates the waveguide where light is launched. (b) Mode excitation amplitude $A(E)$ for initial lattice excitation at the boundary site, i.e., $c_n(0) = \delta_{n,1}$ (c) and (d) Experimental and theoretical maps of the light intensity evolution in the lattice waveguides.

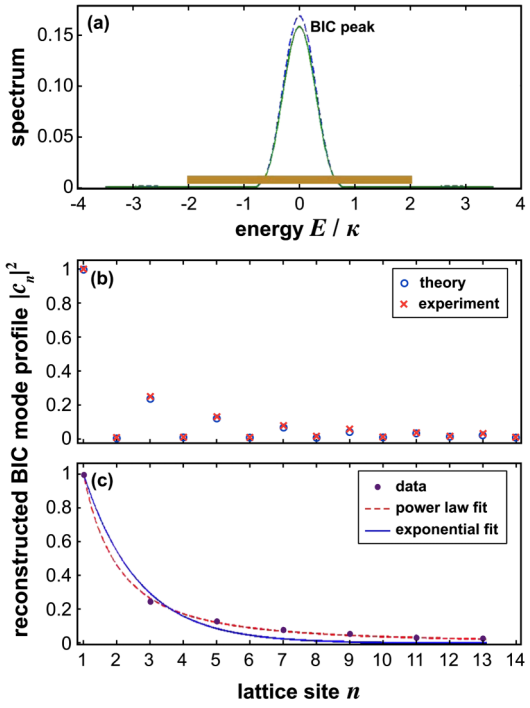

FIG. 3 (color online). (a) Spectrum of the autocorrelation function $|\hat{C}(E)|^2$ versus normalized energy E/κ as obtained from the experimental data (solid curve) and from the theoretical analysis (dashed curve). The solid horizontal line marks the continuous spectrum of the lattice band. The peak at $E = 0$ corresponds to the BIC mode. (b) Reconstructed BIC mode profile $|\bar{c}_n(E = 0)|^2$ (crosses refer to the experimental data, open circles to numerical simulations). (c) Best exponential (solid line) and algebraic (dashed line) fitting curves of $|\bar{c}_n(E = 0)|^2$ at odd lattice sites. The algebraic fitting curve is $|\bar{c}_n|^2 = 1/[(n + 1)/2]^{2\alpha}$ with best fit $\alpha = 0.96$.

the square-wave filter, the Gaussian one avoids the appearance of oscillatory tails in the resonance peak, which might be erroneously attributed to the occurrence of other bound states. The computed spectrum $|\hat{C}(E)|^2$ of the autocorrelation function is shown in Fig. 3(a), clearly indicating a resonance peak at $E = E_1 = 0$, i.e., the existence of a bound state with energy E_1 embedded into the spectrum of scattered states. The outer BOC modes are very weakly excited by the initial wave packet, and thus they are not visible in the spectrum of Fig. 3(a). In Fig. 3(b) we show the behavior of the reconstructed BIC eigenvector, obtained from Eq. (6) with $E = 0$, for lattice sites up to $n = 14$. In this case a square filter $g(t)$ has been used, which provides a slightly better estimate than the Gaussian filter. As expected, the values of $|\bar{c}_n|^2$ of even-number waveguides are very small, whereas $|\bar{c}_n|^2$ at odd-number waveguides shows a slow decay. The results shown in Fig. 3(a) and 3(b) are compared with the theoretical predictions based on Eqs. (5) and (6), where the amplitudes $c_n(t)$ are obtained by numerical integration of the coupled-mode equations rather than from the measured intensity map. To prove the algebraic (rather than exponential) localization of the BIC state, the reconstructed mode amplitudes $|\bar{c}_n|^2$ are fitted, at odd lattice sites, by either an inverse power-law curve $|\bar{c}_n|^2 = 1/[(n + 1)/2]^{2\alpha}$ or by an exponential curve $|\bar{c}_n|^2 = \exp[-\alpha(n - 1)]$ with a single fitting parameter α. The optimal fitting curves, obtained by minimizing the rms deviation, are shown in Fig. 3(c). The algebraic curve turns out to provide a much better rms deviation than the exponential one (rms deviation 0.010 06 vs 0.043 16), with an optimum fitting parameter $\alpha = 0.96$, which deviates from the expected value $\alpha = 1$ by $\sim 4\%$.

In conclusion, we have introduced and experimentally demonstrated a new class of surface bound states with algebraic localization. While exponential localization is ubiquitous for evanescent waves, algebraic localization is found when the lattice sustains bound states with an energy buried in the spectrum of scattered states. Here a design procedure of surface states with algebraic decay has been proposed for a tight-binding lattice model with inhomogeneous hopping rates and demonstrated using optical waveguide arrays. Our results provide the first observation of surface states with algebraic localization in a controllable physical system and are expected to be relevant to other fields, including ultracold atoms in optical lattices, electronic transport in quantum dot chains, and mesoscopic structures, as well as other photonic systems.

This work was supported by the European Union through Project No. FP7-ICT-2011-9-600838 (QWAD—Quantum Waveguides Application and Development).

*Corresponding author.
stefano.longhi@polimi.it

[1] S. G. Davison and M. Steslicka, *Basic Theory of Surface States* (Oxford Science Publications, New York, 1996).
[2] I. E. Tamm, Phys. Z. Sowjetunion **1**, 733 (1932).
[3] W. Shockley, Phys. Rev. **56**, 317 (1939).
[4] P. W. Anderson, Phys. Rev. **109**, 1492 (1958).
[5] T. A. L. Ziman, Phys. Rev. B **26**, 7066 (1982); C. M. Soukoulis, I. Webman, G. S. Grest, and E. N. Economou, Phys. Rev. B **26**, 1838 (1982); Y. Morita and Y. Hatsugai, Phys. Rev. Lett. **79**, 3728 (1997); S.-J. Xiong and S. N. Evangelou, Phys. Rev. B **64**, 113107 (2001).
[6] L. Sanchez-Palencia, D. Clement, P. Lugan, P. Bouyer, G. V. Shlyapnikov, and A. Aspect, Phys. Rev. Lett. **98**, 210401 (2007); J. Billy, V. Josse, Z. Zuo, A. Bernard, B. Hambrecht, P. Lugan, D. Clement, L. Sanchez-Palencia, P. Bouyer, and A. Aspect, Nature (London) **453**, 891 (2008).
[7] J. Pappademos, U. Sukhatme, and A. Pagnamenta, Phys. Rev. A **48**, 3525 (1993).
[8] J. von Neumann and E. Wigner, Z. Phys. **30**, 465 (1929).
[9] F. H. Stillinger and D. R. Herrick, Phys. Rev. A **11**, 446 (1975).
[10] H. Friedrich and D. Wintgen, Phys. Rev. A **31**, 3964 (1985).
[11] L. S. Cederbaum, R. S. Friedman, V. M. Ryaboy, and N. Moiseyev, Phys. Rev. Lett. **90**, 013001 (2003).
[12] F. Capasso, C. Sirtori, J. Faist, D. L. Sivco, S-N. G. Chu, and A. Y. Cho, Nature (London) **358**, 565 (1992).

[13] O. Olendski and L. Mikhailovska, Phys. Rev. B **67**, 035310 (2003).
[14] A. F. Sadreev, E. N. Bulgakov, and I. Rotter, Phys. Rev. B **73**, 235342 (2006).
[15] G. Ordonez, K. Na, and S. Kim, Phys. Rev. A **73**, 022113 (2006).
[16] M. L. Ladron de Guevara and P. A. Orellana, Phys. Rev. B **73**, 205303 (2006).
[17] A. Albo, D. Fekete, and G. Bahir, Phys. Rev. B **85**, 115307 (2012).
[18] J. W. Gonzalez, M. Pacheco, L. Rosales, and P. A. Orellana, Europhys. Lett. **91**, 66001 (2010).
[19] B.-J. Yang, M. S. Bahramy, and N. Nagaosa, Nat. Commun. **4**, 1524 (2013).
[20] J.-M. Zhang, D. Braak, and M. Kollar, Phys. Rev. Lett. **109**, 116405 (2012).
[21] S. Longhi and G. Della Valle, J. Phys. Condens. Matter **25**, 235601 (2013).
[22] S. Longhi, Eur. Phys. J. B **57**, 45 (2007).
[23] D. C. Marinica, A. G. Borisov, and S. V. Shabanov, Phys. Rev. Lett. **100**, 183902 (2008).
[24] E. N. Bulgakov and A. F. Sadreev, Phys. Rev. B **78**, 075105 (2008).
[25] Y. Plotnik, O. Peleg, F. Dreisow, M. Heinrich, S. Nolte, A. Szameit, and M. Segev, Phys. Rev. Lett. **107**, 183901 (2011).
[26] S. Weimann, Y. Xu, R. Keil, A. E. Miroshnichenko, S. Nolte, A. A. Sukhorukov, A. Szameit, and Y. S. Kivshar, arXiv:1304.4699.
[27] M. I. Molina, A. E. Miroshnichenko, and Y. S. Kivshar, Phys. Rev. Lett. **108**, 070401 (2012).
[28] See the Supplemental Material at http://link.aps.org/supplemental/10.1103/PhysRevLett.111.220403 for a detailed description of the properties of the Hamiltonian $\hat{H}$ and of the spectral method.
[29] G. Della Valle, R. Osellame, and P. Laporta, J. Opt. A **11**, 013001 (2009).
[30] A. Crespi, S. Longhi, and R. Osellame, Phys. Rev. Lett. **108**, 163601 (2012).
[31] M. D. Feit, J. A. Fleck, and A. Steiger, J. Comput. Phys. **47**, 412 (1982).
[32] A. Szameit, F. Dreisow, H. Hartung, S. Nolte, A. Tünnermann, and F. Lederer, Appl. Phys. Lett. **90**, 241113 (2007).
[33] G. Corrielli, A. Crespi, G. Della Valle, S. Longhi, and R. Osellame, Nat. Commun. **4**, 1555 (2013).